



Automatika

Journal for Control, Measurement, Electronics, Computing and Communications

ISSN: (Print) (Online) Journal homepage: <https://www.tandfonline.com/loi/taut20>

Newton–Raphson based scalar speed control and optimization of IM

Özcan Otkun

To cite this article: Özcan Otkun (2021) Newton–Raphson based scalar speed control and optimization of IM, *Automatika*, 62:1, 55–64, DOI: [10.1080/00051144.2020.1846322](https://doi.org/10.1080/00051144.2020.1846322)

To link to this article: <https://doi.org/10.1080/00051144.2020.1846322>



© 2020 The Author(s). Published by Informa UK Limited, trading as Taylor & Francis Group



Published online: 30 Nov 2020.



Submit your article to this journal [↗](#)



Article views: 193



View related articles [↗](#)



View Crossmark data [↗](#)



Newton–Raphson based scalar speed control and optimization of IM

Özcan Otkun

Department of Electrical and Electronics Engineering, 3Nokta Academy Company, Trabzon, Turkey

ABSTRACT

In this study, Newton–Raphson Based (NRB) scalar speed control (SSC) is recommended to control the speed of Induction Motors (IM). As is known, the Newton–Raphson method, which is often used in numerical analysis, is one of the methods that provide a rapid convergence of the desired value. In this study, the frequency value required for the desired speed value is calculated by Newton–Raphson method. Three different models including Newton–Raphson Based + Scalar Speed Control (NRB_SSC), Difference Speed + NRB_SSC (DS_NRB_SSC), DS + NRB_SSC + Difference Frequency (DS_NRB_SSC_DF) were used for optimization tests. Simulation of the work was done in Matlab/Simulink programme. According to obtained test results DS_NRB_SSC_DF has produced better results.

KEYWORDS

IM; Newton Raphson method; scalar control; speed control; optimization

1. Introduction

We observe that IMs are currently being used in many applications [1]. Being durable and inexpensive, requiring minimal maintenance, being easy to manufacture are shown reasons for this situation [2]. However, these motors' parameters that cannot be modelled during the operation make speed and torque control difficult [3]. When looked at the literature, it has been observed that many control methods were developed and the development of methods is still ongoing [4,5].

Scalar and vector control methods are usually used in the control of IMs [4]. It is observed that the vector control method has preferred in many studies due to its better dynamic response [6–8]. However, Scalar Control Method (SCM) has a simple structure and it is easy to apply. SCM is performed by keeping the voltage/frequency (V/f) ratio constant. Thus, the torque of the motor desired to operate at different speeds is kept constant [9–11]. However, when induction motors are operated at low speeds, torque output decreases due to the reduced internal voltage drop and causes such as external load conditions affect the dynamic performance of the motor [12,13].

Proportional, Integral, Derivative (PID) control methods have been developed to improve the performance of scalar and vector control methods [14,15]. PI control method is being used in applications of IM with SCM. So, successful results are obtained for constant speed and torque values [11]. However, changes in speed and torque values disrupt the dynamic stability of PID control [16]. In this case, it is necessary to readjust the parameters of PID [17–19].

Referring to the literature, it is observed that intelligent control systems which can be used instead of the

PID have been developed [20,21]. These methods show the desired performance in the nonlinear case in system [22]. Also, the control performance system is less affected from parameter variations [23–25].

In fact, we see that a mathematical model is used in addition to traditional methods (scalar and vector) in the design of control systems. In this study, performance in the control system of Newton–Raphson Method (NRM) which is used in the solution of nonlinear problems will be examined. In this sense, the aim of the study is to talk about an alternative control method. The goal here is to achieve a similar goal with a different method, not reveal that SCM, PID and intelligent controllers fail. With the method used, the frequency required for the motors to reach the desired speed without load or load will be calculated. Considering the studies conducted so far, it seems that NRM is used for comparison and verification purposes [26]. One of these studies; Pervin et al. [27] have compared current by calculating with traditional methods and NRM in a wide speed ranging and high-performance drivers which are designed for the speed permanent magnet synchronous motor. It is observed that the proposed calculation method is available to use. Merabet et al. [28] have studied on an Artificial Neural Network (ANN) based control algorithm in the speed control of IM. In the proposed method, ANN outcomes were calculated with NRM and compared. They have stated that simulation results can be used in control studies. Shafiq and Khan [29] have performed the numerical analysis of the method which they have proposed in their study on DC motor control with NRM. They have reported that the test results obtained from the simulation could be used on the control of nonlinear systems. Padron

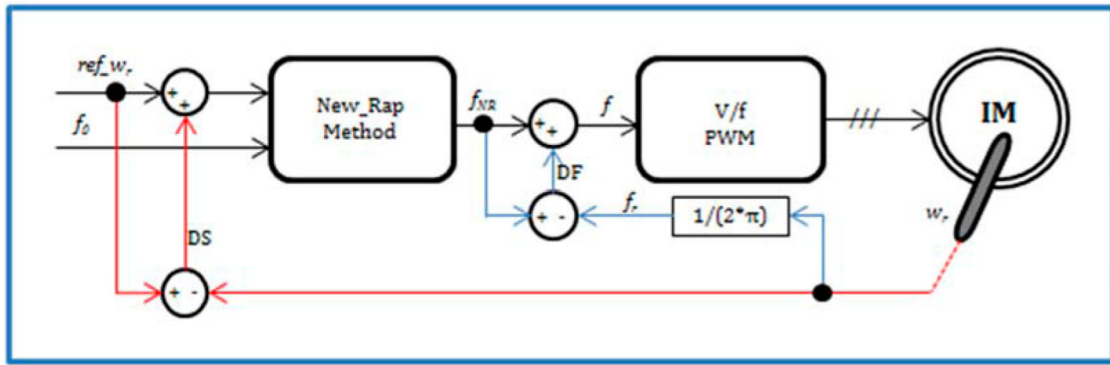


Figure 1. Block circuit diagram of DS_NRB_SSC_DF model.

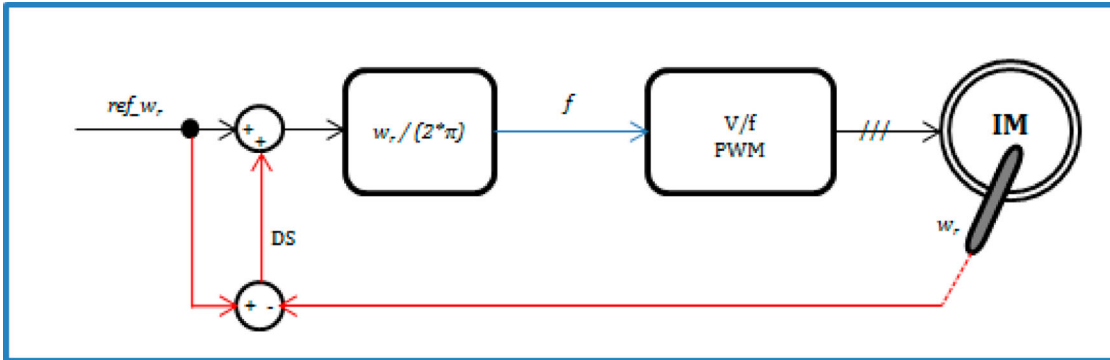


Figure 2. Block circuit diagram of SCM model.

and Lorenzo [30] have studied steady-state analysis of the induction generator. They have used this NRM-based method to obtain the electrical parameters of the machine under certain conditions. Radler et al. [31] have proposed a control system used different algorithms for PID and they have observed that the results are available to use by comparing with NRM. Lin et al.

[32] have stated in their study that NRM can be used in control systems.

In this study, NRM-based SSC is recommended for IMs. The Matlab/Simulink software [33] will be used in simulations of the study. In this context, first, the mathematical expressions of NRM were explained. Then, the mathematical expressions of IM and scalar control

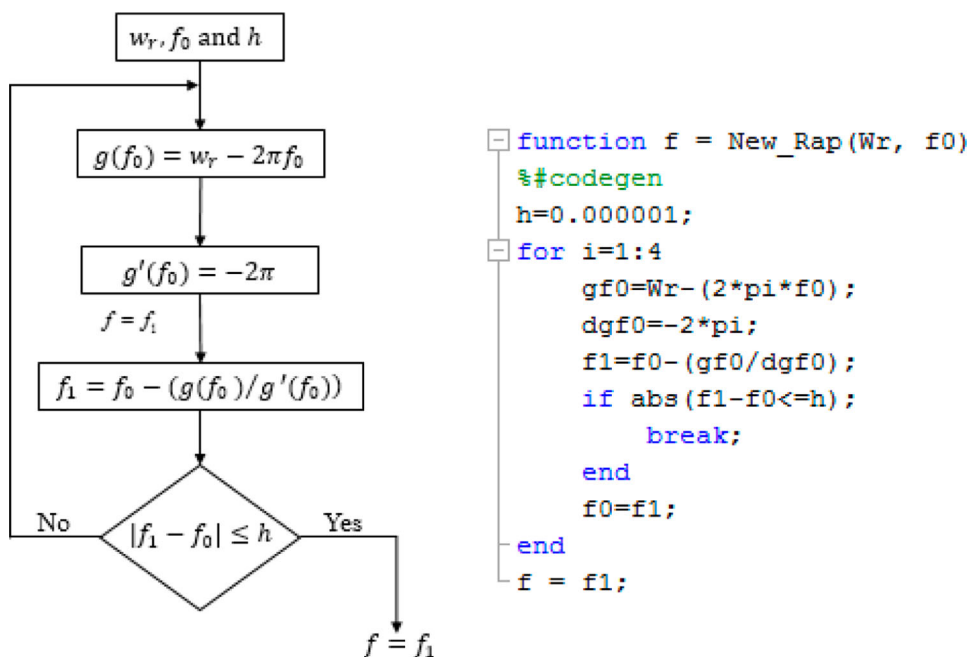


Figure 3. Flow diagram and matlab function block software.

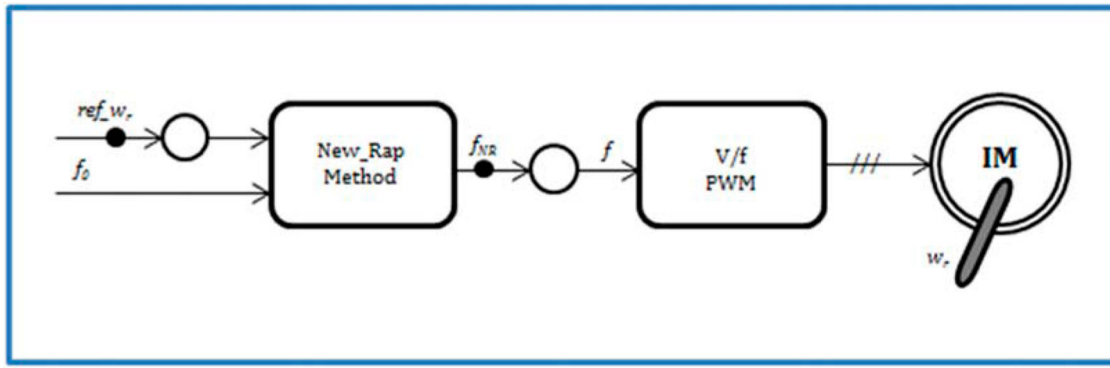


Figure 4. Block diagram of NRB_SSC.

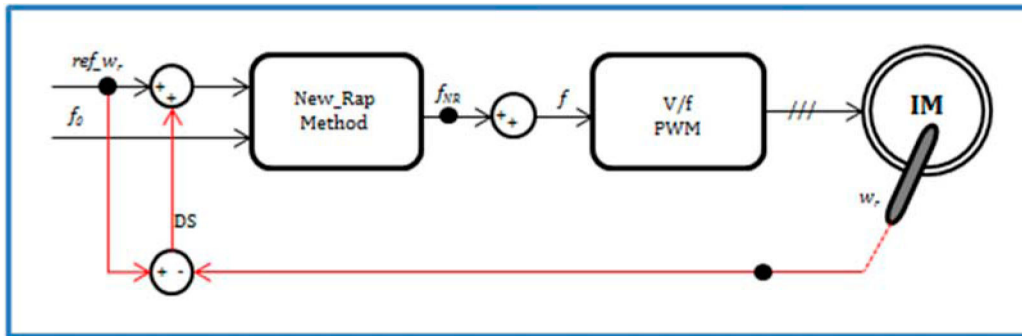


Figure 5. Block diagram of DS_NRB_SSC.

are given. Simulation and test results are presented in graphs and tablet.

2. Materials and methods

Block circuit diagram of the proposed speed control in this study are shown in Figure 1. Wherein the speed of the IM is achieved by changing the frequency.

Since SCM is designed according to the constant motor parameters, it is unsatisfactory for changing motor parameters and different load conditions during operation [13]. Therefore, NRM which is the most widely known numerical analysis of nonlinear systems

Table 1. Test values.

w_r (rpm)	T_{L0} (Nm)	T_{L1} (Nm)	T_{L2} (Nm)
10	0	0.5	1
30	0	0.5	1
50	0	0.5	1

has been used as the speed controller in the control structure. The NRM will provide the required output frequency for the desired speed of IM under varying load conditions. The reference speed and the initial frequency (0.1 Hz) will be used as input variables. As shown in Figure 1, Difference Speed (DS) (speed error)

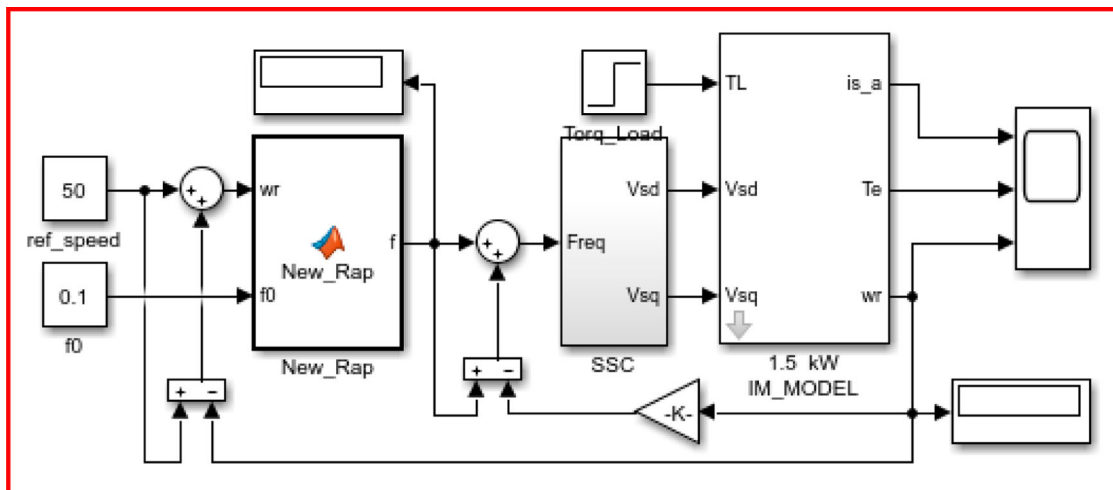


Figure 6. The simulation model of DS_NRB_SSC_DF.

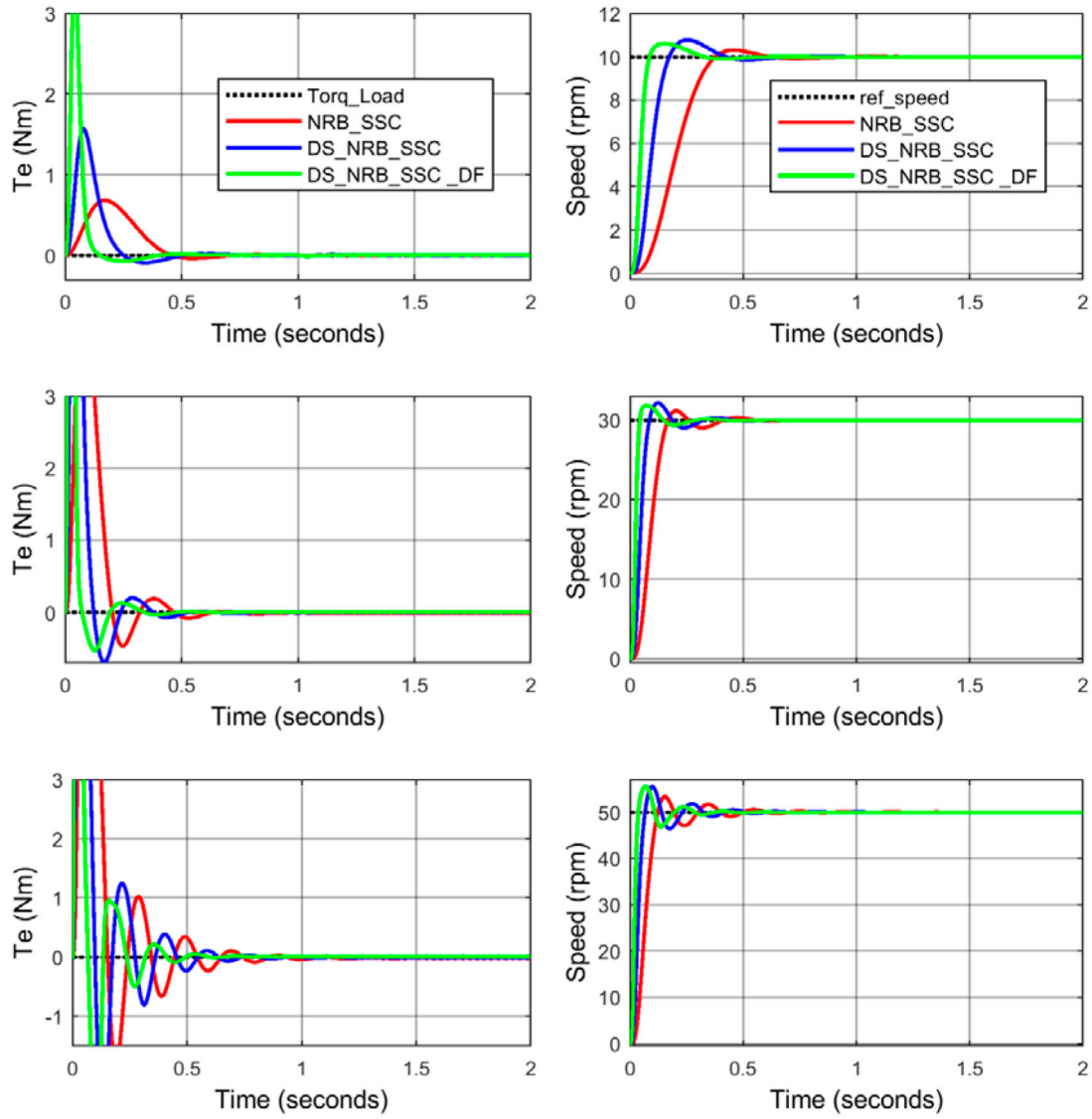


Figure 7. Graphs obtained unloaded condition at 10, 30, 50 rpm, respectively.

and **Difference Frequency (DF)** (frequency error) are given back to the system for optimization of the proposed method. Thus, PI (Proportional, Integral) controller effect has been brought to NRM output and therefore, steady-state errors have been tried to be corrected. The NRB_SSC was used in the speed control structure of IM given in Figure 1 and classic SCM in Figure 2. Mathematical expressions of the motor used in the simulation study and NRB_SSC structure used in the speed control are given below.

2.1. Mathematical expressions of IM

Axis system conversion is needed for analysing the dynamic behaviour of IM. These conversions are shown below.

The conversion of the a - b - c axes system to d - q axes system:

$$\begin{bmatrix} s_d \\ s_q \end{bmatrix} = \frac{2}{3} \begin{bmatrix} \cos(\theta) & \cos(\theta - (2\pi/3)) \\ -\sin(\theta) & -\sin(\theta - (2\pi/3)) \end{bmatrix}$$

$$\begin{bmatrix} \cos(\theta + (2\pi/3)) \\ -\sin(\theta + (2\pi/3)) \end{bmatrix} \begin{bmatrix} s_a \\ s_b \\ s_c \end{bmatrix} \quad (1)$$

The conversion of the d - q axes system to a - b - c axes system:

$$\begin{bmatrix} s_a \\ s_b \\ s_c \end{bmatrix} = \frac{2}{3} \begin{bmatrix} \cos(\theta) & -\sin(\theta) \\ \cos(\theta - (2\pi/3)) & -\sin(\theta - (2\pi/3)) \\ \cos(\theta + (2\pi/3)) & -\sin(\theta + (2\pi/3)) \end{bmatrix} \times \begin{bmatrix} s_d \\ s_q \end{bmatrix} \quad (2)$$

Parameter s in Equations (1) and (2) represents the magnetic flux, the current and voltage. Mathematically equivalent expressions of IM in d - q axes are given below [4].

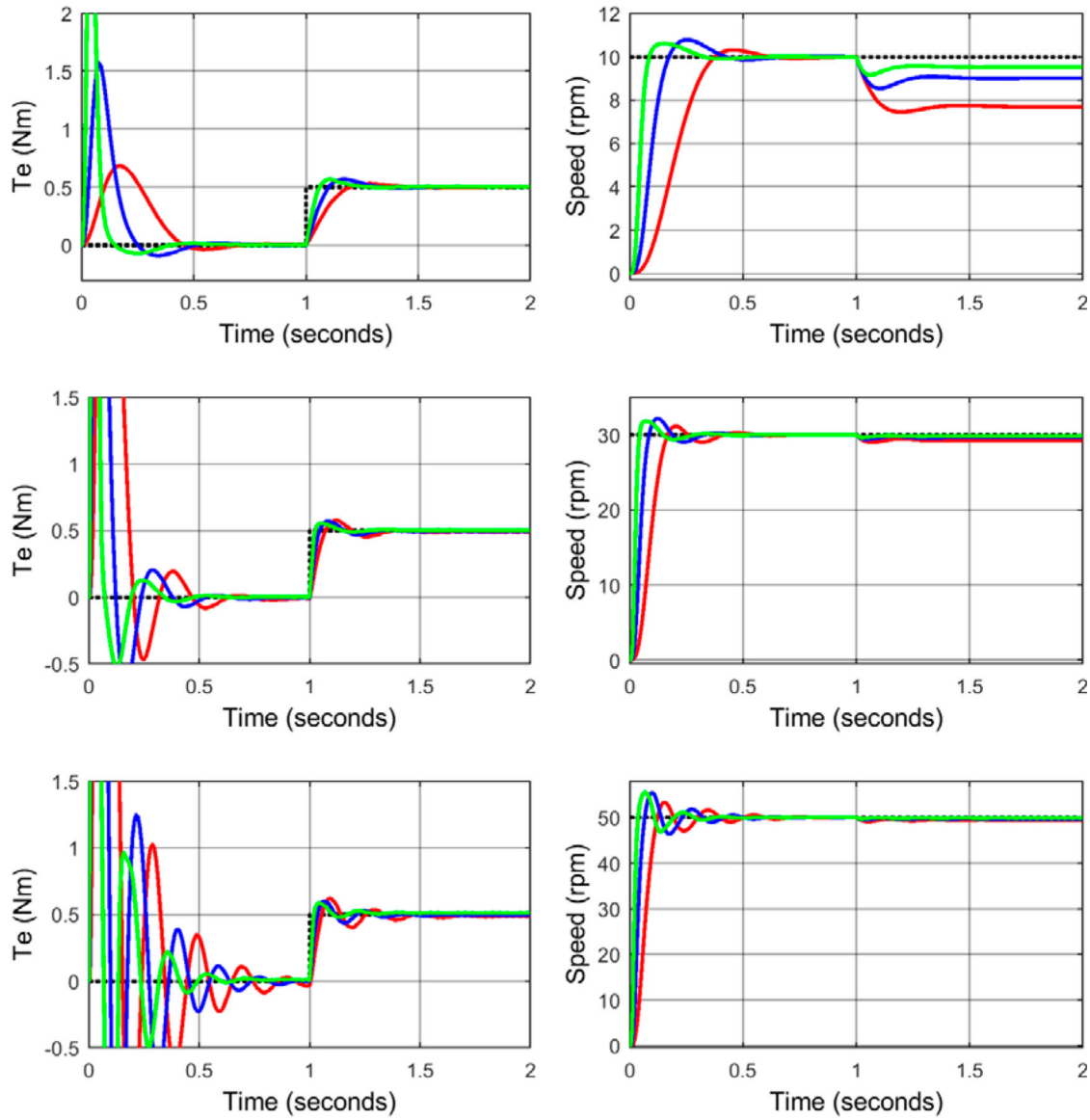


Figure 8. Graphics obtained 0.5 Nm load at 10, 30, 50 rpm, respectively.

Magnetic Flux Equations;

$$\begin{aligned}
 \psi_{ds} &= \int (v_{ds} - i_{ds}R_s)dt \\
 \psi_{qs} &= \int (v_{qs} - i_{qs}R_s)dt \\
 \psi_{dr} &= - \int (w_r\psi_{qr} + i_{dr}R_r)dt \\
 \psi_{qr} &= \int (w_r\psi_{dr} + i_{qr}R_r)dt
 \end{aligned} \tag{3}$$

Current Equations;

$$\begin{aligned}
 i_{ds} &= (\psi_{ds} - \psi_{dr}(L_m/L_r))(1/(L_s - (L_m^2/L_r))) \\
 i_{qs} &= (\psi_{qs} - \psi_{qr}(L_m/L_r))(1/(L_s - (L_m^2/L_r))) \\
 i_{dr} &= (\psi_{dr} - \psi_{ds}(L_m/L_r))(1/(L_r - (L_m^2/L_r))) \\
 i_{qr} &= (\psi_{qr} - \psi_{qs}(L_m/L_r))(1/(L_r - (L_m^2/L_r)))
 \end{aligned} \tag{4}$$

Electromagnetic Torque Equations;

$$T_e = \frac{3p}{4}(\psi_{ds}i_{qs} - \psi_{qs}i_{ds}) \tag{5}$$

Speed Equations;

$$w_r = \frac{p}{2} \int (T_e - T_L) \frac{1}{j} dt \tag{6}$$

or

$$w_r = 2\pi f_r \tag{7}$$

In these equations; Ψ : Stator (s) and rotor (r) flux in d - q axes, v : Stator (s) and rotor (r) voltages in d - q axes, i : Stator (s) and rotor (r) currents in d - q axes, w_r : Rotor speed (resultant speed), R_{s-r} : Stator (s) and rotor (r) resistance, L_{s-r} : Stator (s) and rotor (r) inductance, L_m : Mutual inductance, p : Number of poles, T_L : Load torque, j : Inertia, f : The frequency. Simulation performed motor parameters of IM are $R_s = 4.85 \Omega$, $R_r = 3.81 \Omega$, $L_s = L_r = 0.274$ H, $L_m = 0.258$ H, $j = 0.031$ kg m², $P = 1.5$ kW, $p = 4$.

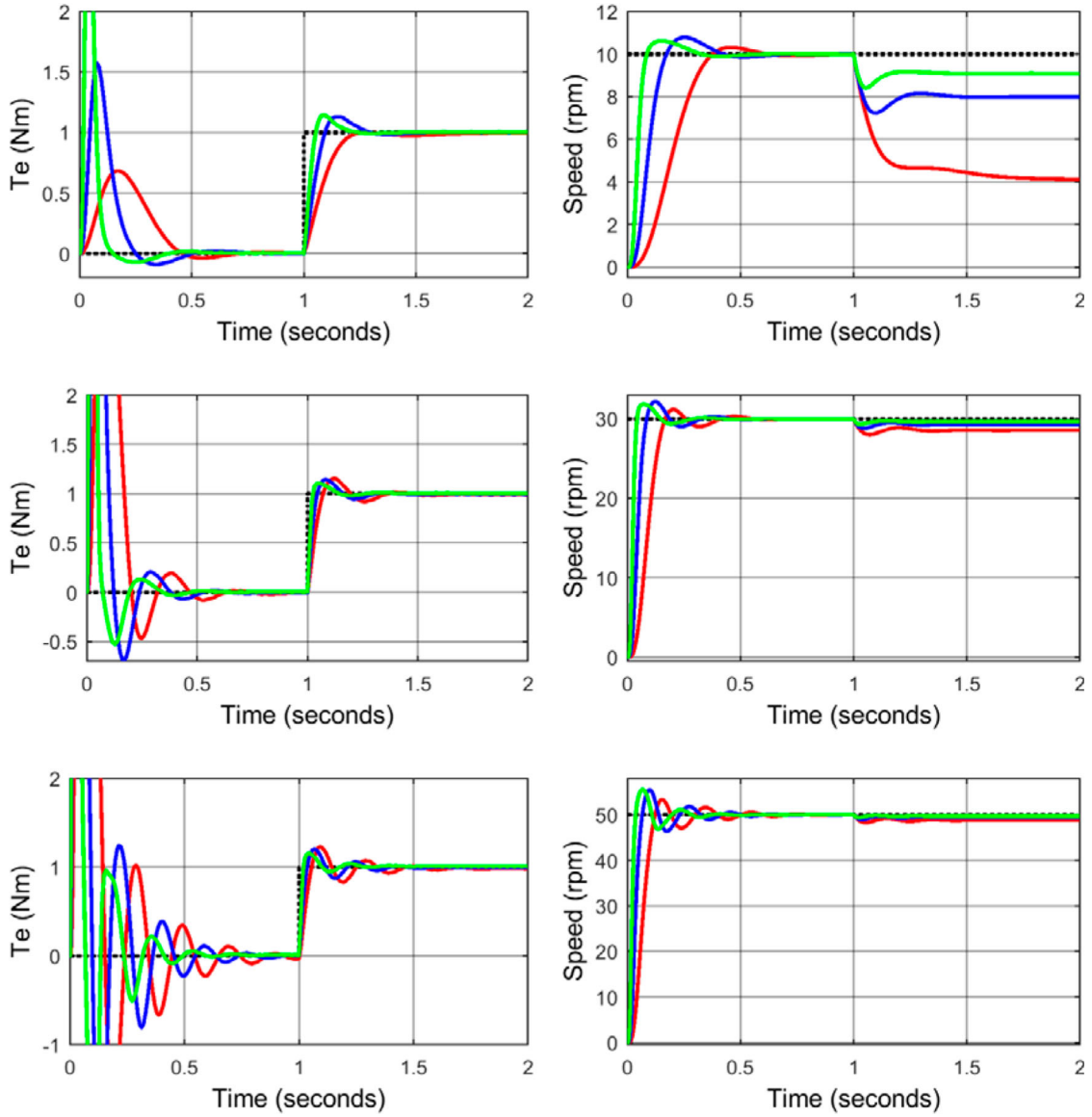


Figure 9. Graphics obtained 1 Nm load at 10, 30, 50 rpm, respectively.

2.2. NRB_SSC structure

NRM is the method used in finding the roots of non-linear equations. An approximate root of the equation is determined with an error caused by the approach. In this method, corrected value of the root is equal to the sum of the error and the approximate root [34].

$$x_1 = x_0 + h \quad (7)$$

Here, x_0 indicates the approximate root, h indicates approximation error and x_1 indicates the corrected root. Wherein, if x_1 is assumed to be the root of $f(x)$,

$$f(x_1) = f(x_0 + h) = 0 \quad (8)$$

If $f(x_0 + h)$ is opened in the Taylor series,

$$f(x_0 + h) = f(x_0) + \frac{h}{1!}f'(x_0) + \frac{h^2}{2!}f''(x_0) + \dots \quad (9)$$

By taking the first two terms,

$$f(x_1) = f(x_0 + h) = f(x_0) + hf'(x_0) \quad (10)$$

Here, since x is a root of $f(x)$,

$$\begin{aligned} f(x_0) + hf'(x_0) &= 0 \\ h &\cong -f(x_0)/f'(x_0) = x_1 - x_0 \end{aligned} \quad (11)$$

Here is a new root,

$$\begin{aligned} x_1 &= x_0 - (f(x_0)/f'(x_0)) \\ x_2 &= x_1 - (f(x_1)/f'(x_1)) \\ &\vdots \\ x_{n+1} &= x_n - (f(x_n)/f'(x_n)) \end{aligned} \quad (12)$$

$|x_{n+1} - x_n| \leq h$ value is controlled in each step. If the condition occurs, the iteration is finished. With the help of given equations NRB_SSC was carried out with 7th Equation. Equations in 13th were obtained with the help of Equation 7.

$$\begin{aligned} 0 &= w_r - 2\pi f = g(f) \\ g'(f) &= -2\pi \end{aligned} \quad (13)$$

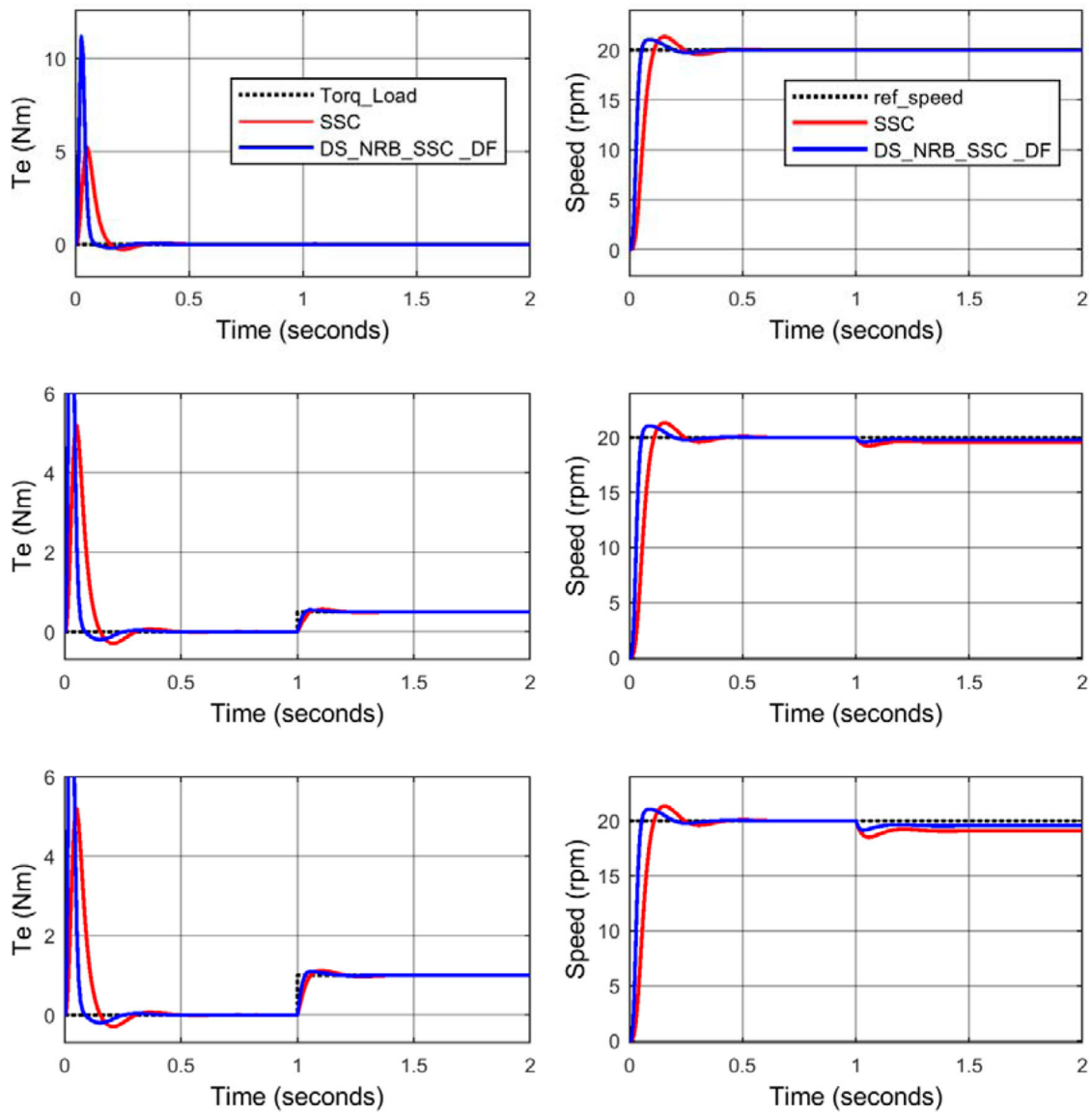


Figure 10. Graphics obtained 20 rpm speed at 0, 0.5, 1 Nm load torque, respectively.

Thus, the general equation of NRM,

$$f_{n+1} = f_n - (g(f_n)/g'(f_n)) \quad (14)$$

In this case, the algorithm steps of NRM;

- Determine the desired speed value (w_r), a random initial value (f_0) and the margin of error (h),
- Calculate $g(f_0)$ and $g'(f_0)$,
- Calculate $f_1 = f_0 - (g(f_0)/g'(f_0))$,
- If $|f_1 - f_0| \leq h$ is not provided then make $f_0 = f_1$ and get back to step 2,
- Result is (f).

Signal flow diagram for the given algorithm and Matlab function block software is shown in Figure 3.

The frequency obtained from NRM output is sent to the SCM block. The mathematical expressions used for

the SCM simulation are given in Equation 15.

$$\begin{aligned} v_a &= v_m \sin(\theta) \\ v_b &= v_m \sin(\theta - (2\pi/3)) \\ v_c &= v_m \sin(\theta + (2\pi/3)) \end{aligned} \quad (15)$$

2.3. Designed controllers

Three different models were tested by simulation studies for NRB_SSC optimization.

- The first model (NRB_SSC) (First Case): The model block diagram is shown in Figure 4.
- The second model (DS_NRB_SSC) (Second Case): The model block diagram is shown in Figure 5.
- The third model (DS_NRB_SSC_DF) (Third Case): the block diagram of the model shown in Figure 1. The simulation model of this study is shown in Figure 6.

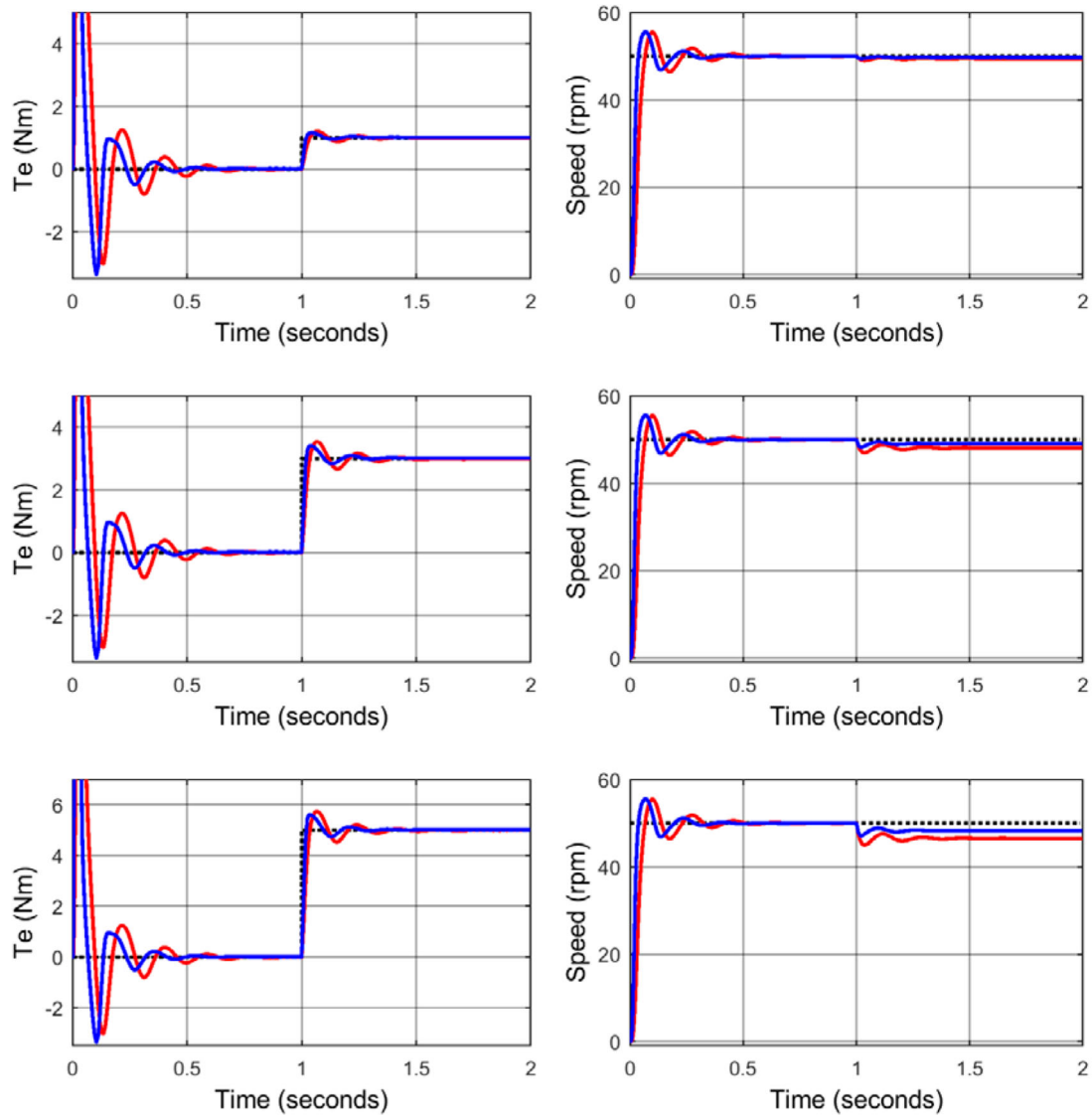


Figure 11. Graphics obtained 50 rpm speed at 1, 3, 5 Nm load torque, respectively.

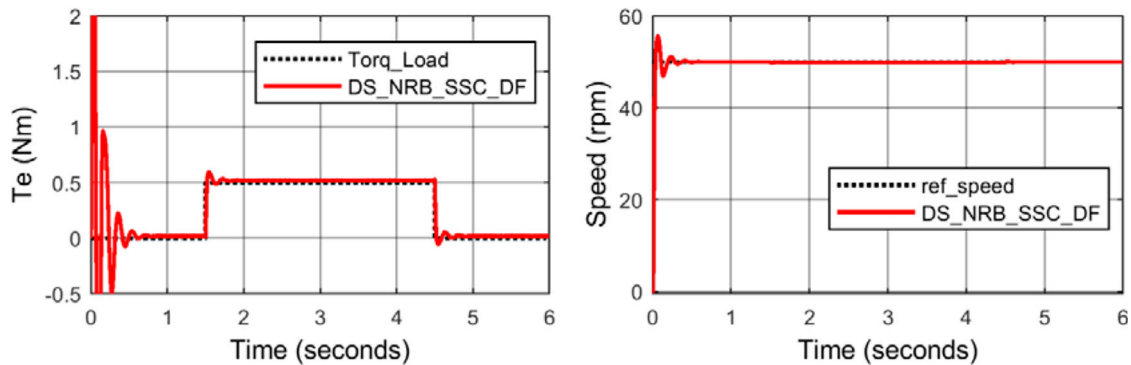


Figure 12. Graphs of variable torque and constant speed.

3. Simulation and test results

Test values used in the simulation are shown in Table 1. Since SSC is not showing desired performance at low speeds, tests were carried out at 50 rpm and lower speed.

Given simulation results indicate the flow of the torque and speed respectively. ASM test results are

obtained depending on the load torque. Obtained test results are presented for benchmarking together in Figures 7–9.

For example, Figure 8 includes graphs obtained in 10, 20 and 30 rpm. Occurred current, torque and speed graphics are seen respectively at the desired speed values for 0.5 Nm load.

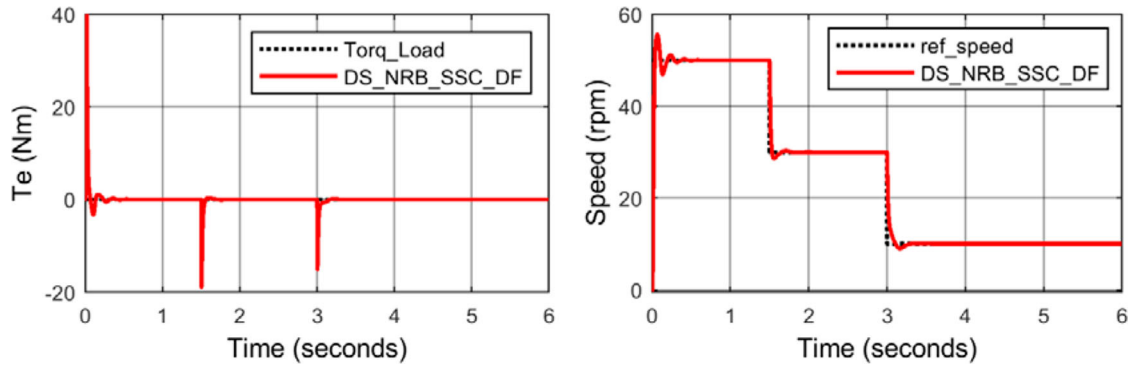


Figure 13. A constant torque and variable speed graphs.

Table 2. The obtained data.

T_L	w_r	First model	% Error	Second model	% Error	Third model	% Error
0	10	9.99	0.10%	9.99	0.10%	9.99	0.10%
	30	30	0.00%	30	0.00%	30	0.00%
	50	50	0.00%	50	0.00%	50	0.00%
0.5	10	7.68	23.20%	9.01	9.90%	9.53	4.70%
	30	29.32	2.27%	29.66	1.13%	29.83	0.57%
	50	49.44	1.12%	49.72	0.56%	49.86	0.28%
1	10	4.12	58.80%	7.99	20.10%	9.09	9.10%
	30	28.57	4.77%	29.3	2.33%	29.65	1.17%
	50	48.85	2.30%	49.43	1.14%	49.72	0.56%

The results obtained from the SSC and the proposed NRB_SSC are given in Figures 10 and 11. When the graphs are analysed, it is seen that NRB_SSC produces positive results.

In addition, graphs of variable torque and constant speed tested for this study are shown in Figure 12. A constant torque and variable speed graphs are shown in Figure 13.

Data belonging to these graphs are given in Table 2, collectively. According to the table given above:

- In the first model; for 10 rpm, it has produced successful results in the unloaded condition only. It has been observed that it has not produced successful results for 0.5 and 1 Nm load with 23.2% and 58.8% error percentages respectively. For 30 rpm, it has been successful in the unloaded condition. However, it has been seen that it made 2.27% and 4.77% errors at 0.5 and 1 Nm load respectively. For 50 rpm, it has been successful in the unloaded condition. However, it has been seen that it has made 1.12% and 2.3% errors at 0.5 and 1 Nm load respectively.
- In the second model; for 10 rpm, it has produced successful results in the unloaded condition only. It has been observed that it has not produced successful results for 0.5 and 1 Nm load with 9.9% and 23.1% error percentages respectively. For 30 rpm, it has been successful in the unloaded condition. However, it has been seen that it made 1.13% and 2.33% errors at 0.5 and 1 Nm load respectively. For 50 rpm, it has been successful in the unloaded condition.

However, it has been seen that it has made 0.56% and 1.14% errors at 0.5 and 1 Nm load respectively.

- In the third model; for 10 rpm, it has produced successful results in the unloaded condition. It has been observed that it has not produced successful results for 0.5 and 1 Nm load with 4.7% and 9.1% error percentages respectively. For 30 rpm, it has been successful in the unloaded condition. However, it has been seen that it made 0.57% and 1.17% errors at 0.5 and 1 Nm load respectively. For 50 rpm, it has been successful in the unloaded condition. However, it has been seen that it has made 0.28% and 0.56% errors at 0.5 and 1 Nm load respectively.

4. Conclusion

In this study, NRB_SSC was carried out for the speed control of IM. The proposed method is explained in detail in the application of motor speed control, and the performances of the designed controllers are graphically shown. Three different methods, at three different loads and three different speed values for each were tested in the study. According to the obtained results;

- Successful results were obtained from all models while IM was unloaded.
- While all models were successful in 30 and 50 rpm at 0.5 Nm load, for 10 rpm a successful result was obtained only from the DS_NRB_SSC_DF.
- All models were successful for 30 and 50 rpm at 1 Nm load but at 10 rpm unsatisfactory results were obtained from all models.
- The most successful results were obtained from the DS_NRB_SSC_DF model in all models at 0.5 and 1 Nm loads.

Based on these results; the performance criteria of the proposed method is seen to be quite successful. This developed application is applicable to experimental studies for research purposes. Because studies have been active research in many countries this study is also expected to contribute to the literature.

Disclosure statement

No potential conflict of interest was reported by the author(s).

ORCID

Özcan Otkun  <http://orcid.org/0000-0002-5025-1516>

References

- [1] Wildi T. *Electrical machines, drives and power systems*. New Jersey: Prentice Hall; 2002.
- [2] Muenchhof M, Beck M, Isermann R. Fault-tolerant actuators and drives – structures, fault detection principles and applications. *Annu Rev Control*. 2009;33(2): 136–148.
- [3] Yahi A, Barazane L. Application of fuzzy sliding approach for speed control in field oriented process and to reduce chattering of an induction motor. *J Electr Eng*. 2014;14(1):1–7.
- [4] Abu-Rub H, Iqbal A, Guzinski J. High performance control of AC drives with MATLAB/simulink models. West Sussex: Wiley; 2012.
- [5] Krause P, Wasynczuk O, Sudhoff S, et al. *Analysis of electric machinery and drive systems*. New Jersey: Wiley; 2013.
- [6] Gunabalan R, Subbiah V. single inverter fed speed sensorless vector control of parallel connected two motor drive. *Automatika*. 2016;57(2):416–427.
- [7] Sahoo SK, Bhattacharya T. Rotor flux-oriented control of induction motor with synchronized sinusoidal PWM for traction application. *IEEE Trans Power Electron*. 2016;31(6):4429–4439.
- [8] Kim SH, Sul SK. Maximum torque control of an induction machine in the field weakening region. *IEEE Transact Indust Appl*. 1995;31(4):787–794.
- [9] Bose BK. *Power electronics and variable frequency drives*. New York: IEEE Press; 1996.
- [10] Oteafy A, Chiasson J. A study of the Lyapunov stability of an open-loop induction machine. *IEEE Trans Control Syst Technol*. 2010;18(6):1469–1476.
- [11] Suetake M, Silva IN, Goedel A. Embedded DSP-based compact fuzzy system and its application for induction-motor V/f speed control. *IEEE Trans Ind Electron*. 2011;58(3):750–760.
- [12] El-Saady G, Sharaf AM, Makky A, et al. A high performance induction motor drive system using fuzzy logic controller. *Proceedings of the 7th Mediterranean Electrotechnical Conference, Antalya, Turkey; 1994*, 1058–1061.
- [13] Senthilkumar S, Vijayan S. High performance Emotional intelligent controller for induction motor speed control. *J Intell Fuzzy Syst*. 2014;27(2):891–900.
- [14] Krishnan R. *Electric motor drives-modeling, analysis, and control*. Upper Saddle River: Prentice-Hall; 2001.
- [15] Türkmenoğlu V, Aktaş M, Karataş S, et al. Soft Set-based Switching Faults Decision Making in DTC induction motor Drives. *J Circuits Syst Comput*. 2015;24(2):1–14.
- [16] Otkun Ö, Doğan RÖ, Akpınar AS. Neural Network based scalar speed control Of Linear permanent magnet synchronous motor. *J Faculty Eng Architect Gazi Univ*. 2015;30(3):395–404.
- [17] Deng J, Tu L. Improvement of direct torque control low-speed performance by using fuzzy logic technique. *Proceedings of the IEEE International Conference on, Mechatronics and Automation Luoyang, Henan; 2006*. 2481–2485.
- [18] Sabir A, Kassar M. A novel and simple hybrid fuzzy/PI controller for brushless DC motor drives. *Automatika*. 2015;56(4):424–435.
- [19] Senthilkumar S, Vijayan S. Impact of using a novel emotional intelligent controller for induction motor speed control. *J Test Eval*. 2013;42(3):1–15.
- [20] Douiri MR, Belghazi O, Cherkaoui M. Recurrent self-tuning neuro-fuzzy for speed induction motor drive. *J Circuits Syst Comput*. 2015;24(9): 1550131 (16 pages).
- [21] Ustun SV, Demirtaş M. Optimal tuning of PI coefficients by using fuzzygenetic for V/f controlled induction motor. *Expert Syst Appl*. 2008;34(4):2714–2720.
- [22] Chen C, Lai C, Sun W. Fuzzy Testing for Regression Coefficient of Fuzzy Numbers. *J Test Eval*. 2012;41(1): 1–6.
- [23] Orłowska-Kowalska T, Blaabjerg F, Rodríguez J. *Advanced and intelligent control in power electronics and drives*. New York: Springer; 2014.
- [24] Krim S, Gdaim S, Mtibaa A, et al. Design and implementation of direct torque control based on an intelligent technique of induction motor on FPGA. *J Electr Eng Technol*. 2015;10(4):30–40.
- [25] Shun-Yuan W, Chwan-Lu T, Shou-Chuang L, et al. An adaptive supervisory sliding fuzzy cerebellar model articulation controller for sensorless vector-controlled induction motor drive systems. *Sensors*. 2015;15(4): 7323–7348.
- [26] Asghari B, Dinavahi V. Novel transmission line modeling method for nonlinear permeance network based simulation of induction machines. *IEEE Trans Magn*. 2011;47(8):2100–2108.
- [27] Pervin S, Siri Z, Uddin MN. Newton-Raphson based computation of id in the field weakening region of IPM motor incorporating the stator resistance to improve the performance. *IEEE Indust Appl Soc Annual Meet*. 2012;6:1–6.
- [28] Merabet A, Ouhrouche M, Bui RT. Neural generalized predictive control with reference control model for an induction motor drive. *Control Intell Syst*. 2008;36:144–152.
- [29] Shafiq M, Khan T. Newton-Raphson based adaptive inverse control scheme for tracking of nonlinear dynamic plants. *1st International Symposium on Systems & Control in Aerospace & Astronautics, Harbin; 2006*, 1343.
- [30] Padrón JFM, Lorenzo AEF. Calculating steady-state operating conditions for doubly-fed induction generator wind turbines. *IEEE Transact Power Syst*. 2010;5(2):922–928.
- [31] Rad AB, Lo WL, Tsang KM. Self-tuning PID controller using Newton–Raphson search method. *IEEE Trans Ind Electron*. 1997;44(5):717–725.
- [32] Lin T, Owens DH, Hatonen J. Newton method based iterative learning control for discrete non-linear systems. *Int J Control*. 2006;79(10):1263–1276.
- [33] CVX Research. CVX: Matlab software for disciplined convex programming, version 2.1 beta. [cited June 2015]. <http://cvxr.com/cvx>.
- [34] Butenko S, Pardalos PM. *Numerical methods and optimization an Introduction*. Boca Raton: CRC Press; 2014.